



Brain accumulation of the EML4-ALK inhibitor ceritinib is restricted by P-glycoprotein (P-GP/ABCB1) and breast cancer resistance protein (BCRP/ABCG2)

Anita Kort^{a,c}, Rolf W. Sparidans^b, Els Wagenaar^a, Jos H. Beijnen^{b,c,d}, Alfred H. Schinkel^{a,*}

^a Division of Molecular Oncology, The Netherlands Cancer Institute, Plesmanlaan 121, 1066CX Amsterdam, The Netherlands

^b Division of Pharmacoepidemiology & Clinical Pharmacology, Department of Pharmaceutical Sciences, Faculty of Science, Utrecht University, Universiteitsweg 99, 3584CG Utrecht, The Netherlands

^c Department of Pharmacy & Pharmacology, The Netherlands Cancer Institute—Antoni van Leeuwenhoek, Plesmanlaan 121, 1066CX Amsterdam, The Netherlands

^d Department of Clinical Pharmacology, The Netherlands Cancer Institute, Plesmanlaan 121, 1066CX Amsterdam, The Netherlands

ARTICLE INFO

Article history:

Received 21 July 2015

Received in revised form 4 September 2015

Accepted 4 September 2015

Available online 8 September 2015

Keywords:

Ceritinib

ALK inhibitor

ABCB1

ABCG2

Blood-brain barrier

Oral availability

ABSTRACT

We aimed to clarify the roles of the multidrug transporters ABCB1 and ABCG2 in oral availability and brain accumulation of ceritinib, an oral anaplastic lymphoma kinase (ALK) inhibitor used to treat metastatic non-small cell lung cancer (NSCLC) after progression on crizotinib. Importantly, NSCLC is prone to form brain metastases. Transport of ceritinib by human (h) ABCB1 or hABCG2 or mouse (m) Abcg2 was assessed *in vitro*. To study the single and combined roles of Abcb1a/1b and Abcg2 in ceritinib disposition *in vivo*, we used appropriate knockout mouse strains. Ceritinib was very efficiently transported by hABCB1, and efficiently by hABCG2 and mAbcg2 *in vitro*, and transport was specifically inhibited by the ABCB1 inhibitor zosuquidar and ABCG2 inhibitor Ko143, respectively. Absorption and 24-h oral availability were not significantly affected by the absence of Abcb1 and/or Abcg2, but the brain concentrations were greatly increased (>38-fold) in Abcb1a/1b^{-/-} mice at 3 and 24 h after oral administration of 20 mg/kg ceritinib. The brain concentrations increased another ~3-fold (to >90-fold) in Abcb1a/1b;Abcg2^{-/-} mice, indicating that there was a significant additional effect of Abcg2-mediated transport of ceritinib as well *in vivo*. Overall, brain accumulation, but not the 24-h oral availability of ceritinib were profoundly restricted by Abcb1a/1b and Abcg2, with Abcb1a/1b being the dominant efflux protein. Our data suggest that coadministration of ceritinib with a dual ABCB1 and ABCG2 inhibitor may improve treatment of brain (micro) metastases positioned behind a functionally intact blood-brain barrier, and possibly also of tumors resistant to ceritinib due to ABCB1 or ABCG2 overexpression.

© 2015 Elsevier Ltd. All rights reserved.

1. Introduction

Lung cancer is the most common type of cancer worldwide, with approximately 1.6 million deaths and 1.8 million newly diagnosed cases every year [1]. About 85–90% of these patients are diagnosed

with non-small cell lung cancer (NSCLC). Roughly half of these patients develop brain metastases in due course, while 7% of the patients present with brain metastases at the time of diagnosis [2–4].

Overall, NSCLC patients have been responding poorly to the standard of care, and only patients harboring specific mutations, affecting EGFR, KRAS or MET benefit from targeted therapies [5,6]. In 2007, a fusion between echinoderm microtubule-associated protein like-4 (EML4) and anaplastic lymphoma kinase (ALK), was identified as a new oncogenic driver mutation in NSCLC [7,8]. About 0.5–11.6% of the NSCLC patients harbor the EML4-ALK rearrangement. However, the incidence increases significantly for younger patients, never-smokers and for patients with adenocarcinoma pathology lacking EGFR and KRAS mutations [9].

Abbreviations: ABC, ATP-binding cassette; ALK, anaplastic lymphoma kinase; AUC, area under the plasma concentration-time curve; BBB, blood-brain barrier; BCRP, breast cancer resistance protein; C_{max}, maximum drug concentration in plasma; EML4, echinoderm microtubule-associated protein like-4; MDCKII, Madin–Darby canine kidney type II cell line; NSCLC, non-small cell lung cancer; P-gp, P-glycoprotein; SD, standard deviation; TKI, tyrosine kinase inhibitor; T_{max}, time after administration of a drug to reach maximum plasma concentration.

* Corresponding author. Fax: +31 20 669 1383.

E-mail address: a.schinkel@nki.nl (A.H. Schinkel).

Crizotinib was the first-in-class ALK inhibitor that showed partial responses or stable disease in as much as ~60% of the ALK-positive NSCLC patients [10]. To date, several case reports describe mixed effects of crizotinib on the treatment of brain metastases [11–13]. Furthermore, a retrospective analysis revealed a modest effect of crizotinib activity behind the blood-brain barrier, using data from patients with brain metastases that were included in phase I and II studies with crizotinib [14]. Unfortunately, resistance to crizotinib eventually occurs, often within a year after initiation of the treatment [15,16].

The novel second generation ALK inhibitor ceritinib is more potent than crizotinib *in vitro* and evokes a more durable response *in vivo*, even in patients that have developed crizotinib resistance [17]. The mechanism of action includes inhibition of the hepatocyte growth factor receptor, insulin-like growth factor 1 receptor and the insulin receptor, but the strongest inhibitory activity is against ALK, where ceritinib inhibits ALK autophosphorylation, ALK-mediated phosphorylation of the downstream signaling protein STAT3 and proliferation of ALK-dependent cells [18]. The first clinical study with ceritinib showed similar therapeutic responses relative to crizotinib, but the responses were irrespective of whether these patients were crizotinib naive or resistant [19]. Furthermore, the same study reported shrinkage of brain metastases in response to ceritinib.

We have previously demonstrated that crizotinib brain penetration is restricted by mAbcb1a/1b, but not mAbcg2, in mouse knockout models [20]. Given the remarkable positive results in early clinical trials where ceritinib showed therapeutic activity against, amongst others, various brain metastases, we were particularly interested to examine the mechanisms that may limit the blood-brain barrier (BBB) penetration of ceritinib. Proper insights into this may provide a rationale to support clinical trials focused on the treatment of (micro) metastasis behind a functionally intact BBB. Based on transport and inhibition experiments in Caco2 cells performed for registration of the drug, ceritinib appeared to be a good substrate of ABCB1 and a weak substrate of ABCG2 *in vitro* [21]. The aim of this study was therefore to investigate whether Abcb1 and Abcg2 affect ceritinib pharmacokinetics and whether these transporters restrict the brain penetration of ceritinib, using various transporter knockout mice.

2. Material and methods

2.1. Chemicals

Ceritinib was purchased from Bio-Connect Services (Huissen, The Netherlands). Zosuquidar was from Sequoia Research Products (Pangbourne, UK) and Ko143 was from Tocris Bioscience (Bristol, UK). Methoxyflurane (Metofane®) was from Medical Developments Australia (Melbourne, Australia) and heparin (5000 IU ml⁻¹) was from Leo Pharma (Breda, The Netherlands). Fetal Calf Serum (FCS) was from Sigma-Aldrich Chemie (Taufkirchen, Germany) and Bovine Serum Albumin (BSA) Fraction V was from Roche (Mannheim, Germany). All chemicals used for the bioanalytical assay of ceritinib were of analytical grade and obtained from Sequoia Research Products (Pangbourne, UK). Ibrutinib from Alsachim (Strasbourg, France) was used as an internal standard in LC-MS/MS assays.

2.2. Transport assays

Transepithelial transport assays were performed in triplicate using polarized Madin-Darby Canine Kidney (MDCKII) cell lines transduced with hABCB1, mAbcg2 or (h)ABCG2 cDNA. Cells were handled and cultured in Dulbecco's Modified Eagle's Medium with

10% fetal calf serum as described previously [22]. Briefly, cells were seeded at a density of 2.5×10^5 cells/well on 12-well microporous polycarbonate membrane filters (3.0- μ m pore size, Transwell 3402, Corning Inc., Lowell, MA) and allowed to form an intact polarized monolayer, as described previously [23]. On day 3, cells were preincubated with the relevant inhibitors for 1 h before the start of the assay. Zosuquidar (5 μ M) was added to the culture medium to inhibit endogenous canine Abcb1 in MDCKII-mAbcg2 and -hABCG2 cell lines. The experiment was initiated by replacing the incubation medium from the donor compartment with fresh drug-containing medium. At 2 and 4 h, 50 μ l samples were collected from the acceptor compartment and stored at -30°C prior to analysis. The amount of transported drug was calculated after correction for volume loss due to sampling. Active transport was expressed by the transport ratio (*r*), which is defined as the amount of apically directed transport divided by the amount of basolaterally directed transport at a defined time point.

2.3. Animals

Male wild-type, *Abcb1a/1b*^{-/-} [24], *Abcg2*^{-/-} [25] and *Abcb1a/1b;Abcg2*^{-/-} [26] mice, all of a >99% FVB genetic background and between 9 and 14 weeks of age, were used. The mice were kept in a temperature-controlled environment with a 12-h light/dark cycle and received a high nutrient diet (Transbreed, SDS Diets, Essex, UK) and acidified water *ad libitum*. All mice were housed and handled according to institutional guidelines in compliance with Dutch legislation, and in accordance with the EU Directive 2010/63/EU for animal experiments.

2.4. Drug solutions

Ceritinib was dissolved in DMSO at 20 mg/ml and aliquots were frozen at -30°C . At the day of the experiment ceritinib aliquots were allowed to thaw and mixed with a vehicle mixture of polysorbate 80, ethanol and water till a clear solution was obtained. Subsequently, the solution was further diluted with 5% (w/v) glucose in water to a 2 mg/ml solution. Final proportions (v/v) of the oral solution were: 10% DMSO, 9% polysorbate 80, 5.85% ethanol, 30.15% water and 45% glucose water (5% w/v). Ceritinib was administered orally at a dose of 20 mg/kg (10 μ l/g).

2.5. Plasma and tissue pharmacokinetics of ceritinib

To minimize variation in absorption and decrease the risk of food effects on ceritinib pharmacokinetics, mice were fasted minimally 2 h prior to the start of the experiment. Mice received 20 mg/kg (10 μ l/g) ceritinib solution by oral gavage, using a blunt-ended needle. Blood samples of 50 μ l were taken from the tail vein using heparin-coated capillaries (Sarstedt, Numbrecht, Germany), at 0.5, 1, 2, 4 and 8 h. After 24 h, mice were anesthetized with isoflurane and blood was collected by cardiac puncture. Immediately thereafter, we isolated brain, liver and kidney. The organs were subsequently weighed and stored at -30°C . Before analysis, organs were allowed to thaw and then homogenized in appropriate volumes of 4% (w/v) BSA in water using a FastPrep®-24 device (MP Biomedicals, SA, California, USA). Blood samples were kept on ice before centrifugation at $2100 \times g$ for 6 min at 4°C , the plasma fraction was collected and also stored at -30°C prior to analysis.

2.6. Relative brain accumulation of ceritinib

Mice were fasted 2 h prior to oral administration of 20 mg/kg ceritinib. At 0.25, 0.5, 1 and 2 h, 50 μ l of blood was taken from the tail vein. After 3 h, all mice were anesthetized with isoflurane and blood was collected by cardiac puncture. Immediately thereafter

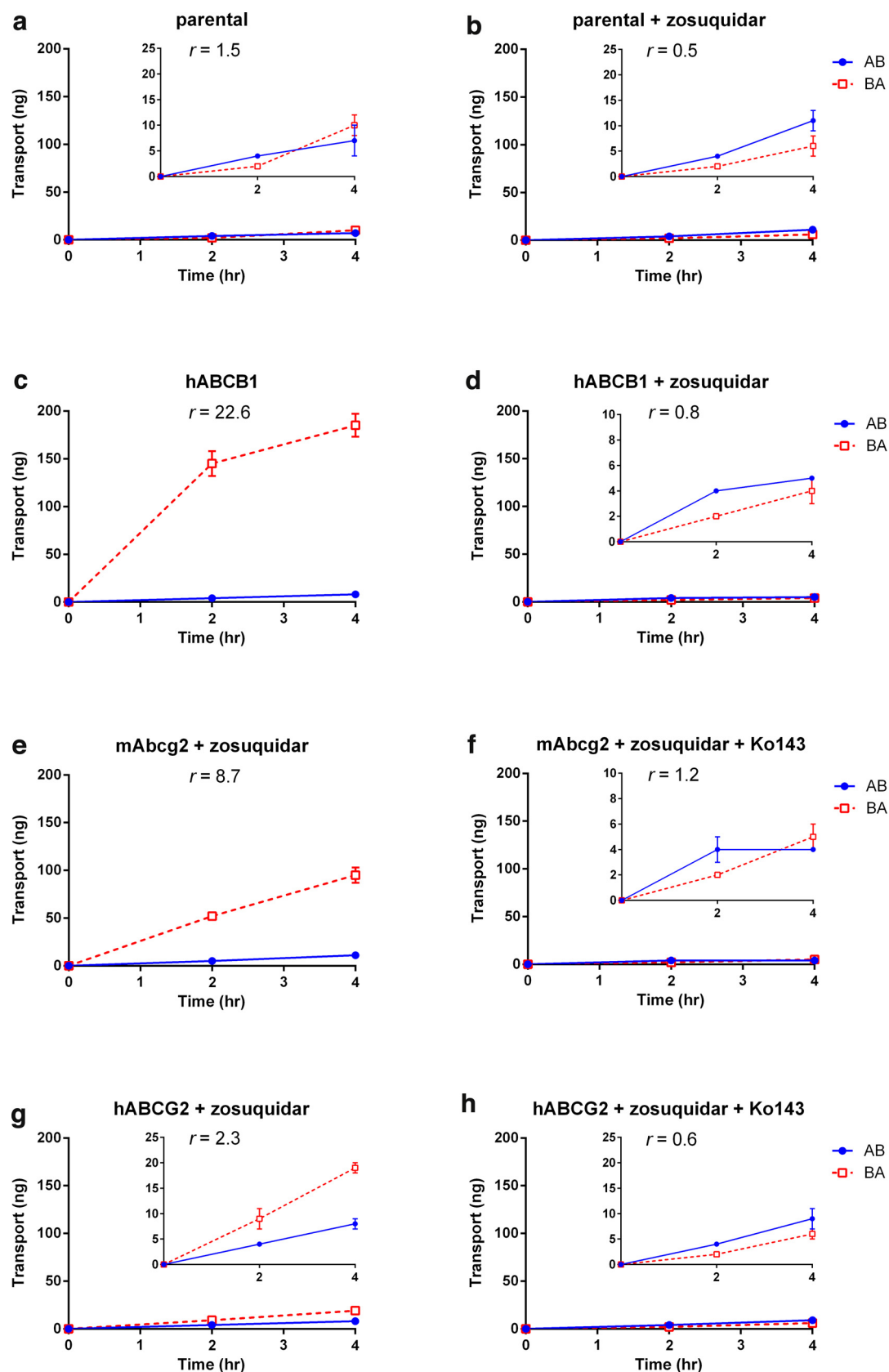


Fig. 1. *In vitro* transport of 5 μ M ceritinib. Transepithelial transport of ceritinib (5 μ M) was assessed in MDCKII cells, either nontransduced parental cells (a, b) or transduced with hABCB1 (c, d), mAbcg2 (e, f) or hABCG2 (g, h) cDNA. At $t = 0$ h, ceritinib was applied to the donor compartment and concentrations in the acceptor compartment were measured at $t = 2$ and 4 h and plotted as total amount of transport (ng) in the graphs. b, d–h: zosuquidar (5 μ M) and/or Ko143 (5 μ M) were applied as indicated, to inhibit hABCB1 or mAbcg2 and hABCG2, respectively. r , Relative transport ratio at 4 h. BA (□, dashed line), translocation from basolateral to apical compartment; AB (●, continuous line), translocation from apical to basolateral compartment. Points, mean ($n = 3$); bars, SD. At $t = 4$ h, 100 ng transport corresponds to an apparent permeability coefficient (P_{app}) of 2.22×10^{-6} cm/s.

mice were sacrificed and brain, liver and kidney were removed and handled as described above. Ceritinib brain concentrations were corrected for the amount of whole blood in brain vascular space (1.4%) [27].

2.7. Drug analysis

Ceritinib concentrations in plasma, tissue homogenates, and cell culture medium were determined by validated sensitive and specific liquid chromatography assays coupled with tandem mass spectrometry (LC–MS/MS) using ibrutinib as internal standard. The calibration range for plasma samples was 5–5000 ng/ml, and 10–10,000 ng/ml for culture medium and tissue homogenates. Full description of the LC–MS/MS method and sample clean up procedure can be found in the supplementary data.

2.8. Statistics and pharmacokinetic calculations

The area under the curve (AUC) of the plasma concentration–time curve was calculated using the trapezoidal rule, without extrapolating to infinity. The peak plasma concentration (C_{\max}) and the time to reach peak plasma concentration (T_{\max}) were determined from individual concentration–time data. One-way analysis of variance (ANOVA) was used to determine significant differences between strains. *Post-hoc* Tukey's multiple comparison test was used to compare significant differences between individual groups. When variances were not homogeneously distributed, data were log-transformed before applying statistical tests. Differences were considered statistically significant when $P < 0.05$. Data are presented as mean \pm SD for 4–6 mice.

3. Results

3.1. Ceritinib is transported very efficiently by hABCB1, and efficiently by mAbcg2 and hABCG2 in vitro

Polarized MDCKII cell lines transduced with hABCB1, mAbcg2 or hABCG2 were used to investigate active transport of 5 μ M ceritinib. We observed only little apically directed transport (from B to A) in the parental MDCKII cell line ($r = 1.5$), but addition of the ABCB1 inhibitor zosuquidar resulted in a clear reduction of apical transport ($r = 0.5$). This may represent inhibition of endogenous canine ABCB1 (Fig. 1a and b). Indeed, there was very pronounced apically directed transport in hABCB1-expressing cells (Fig. 1c, $r = 22.6$), which was efficiently inhibited by zosuquidar (Fig. 1d), indicating that ceritinib is extremely well transported by hABCB1. To abolish any effects of endogenous ABCB1 in ABCG2-expressing cells, we performed transport assays in the presence of zosuquidar. There was clear apically directed transport in the mAbcg2 cell line ($r = 8.7$), which was completely inhibited by Ko143 (Fig. 1e and f, $r = 1.2$). Active transport by hABCG2 was less pronounced ($r = 2.3$), but addition of Ko143 resulted again in a clear inhibition to baseline parental levels (Fig. 1g and h, $r = 0.6$). These data demonstrate that ceritinib was transported extremely well by hABCB1, efficiently by mAbcg2 and modestly by hABCG2 *in vitro*. These transporters might thus potentially play a role in the oral availability and brain penetration of ceritinib.

3.2. Abcb1a/1b and Abcg2 do not affect oral ceritinib absorption or 24-h oral availability

The effect of Abcb1a/1b and Abcg2 on ceritinib plasma pharmacokinetics over 24 h was studied in wild-type, *Abcg2*^{−/−}, *Abcb1a/1b*^{−/−} and *Abcb1a/1b;Abcg2*^{−/−} mice after oral administration of 20 mg/kg ceritinib (Fig. 2a). Ceritinib was slowly absorbed, with an extended T_{\max} range between 2 and 8 h, sometimes even up

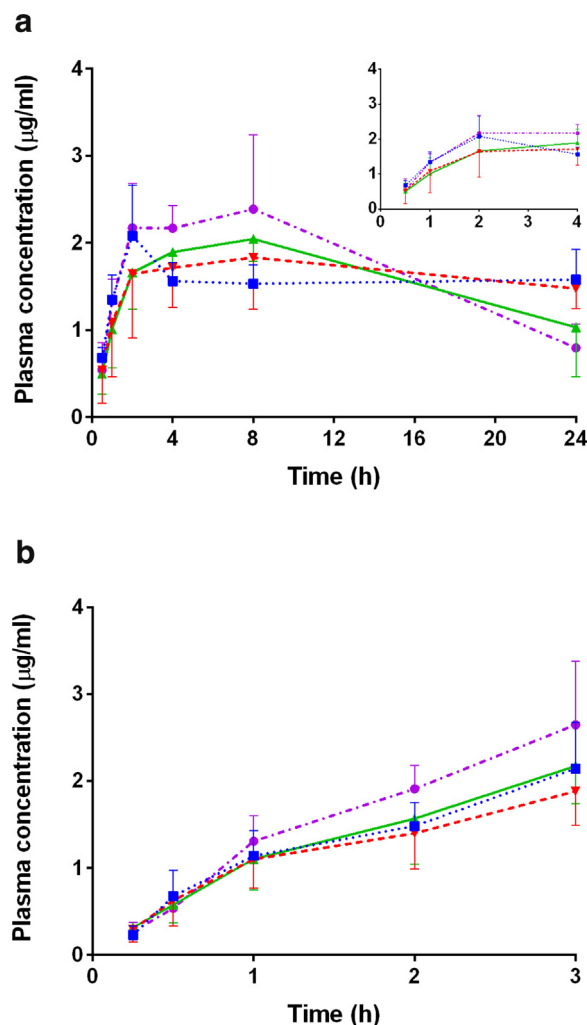


Fig. 2. Plasma concentration–time curves over 24 h (a) and 3 h (b) after oral administration of 20 mg/kg ceritinib to male wild-type (●), *Abcg2*^{−/−} (▲), *Abcb1a/1b*^{−/−} (▼) and *Abcb1a/1b;Abcg2*^{−/−} (■) mice. The inset in panel a shows a representation of the same data up till 4 h, for comparison with panel b. Points, mean ($n = 4–6$); bars, SD.

to 24 h in individual knockout mice. There was no apparent effect of single or combination knockout of *Abcg2* and/or *Abcb1a/1b* on the rate of absorption of ceritinib compared to wild-type mice. This was confirmed by the plasma concentration results obtained in a separate short-term (3 h) tissue accumulation experiment in the same mouse strains (Fig. 2b). The plasma concentration between 8 and 24 h did seem to decrease more slowly for both *Abcb1a/1b*-deficient strains, but this did not result in significant differences in AUCs from wild-type mice (Fig. 2a, Table 1).

3.3. Ceritinib brain penetration is strongly restricted by *Abcb1a/1b* and *Abcg2*

Twenty-four hours after oral administration of ceritinib, mice were sacrificed and ceritinib concentrations in brain, liver and kidney determined. Low levels of ceritinib were readily detectable in wild-type brain after 24 h. A dramatic 62-fold increase in brain concentration compared to wild-type mice was observed for *Abcb1a/1b* knockout mice ($P < 0.001$, Fig. 3a). The absence of *Abcg2* alone had no substantial impact on ceritinib brain penetration. However, when both *Abcb1a/1b* and *Abcg2* were absent, the brain concentration was increased 193-fold compared to wild-type mice, and 3.1-fold compared to *Abcb1a/1b*^{−/−} mice (both $P < 0.001$,

Table 1
Pharmacokinetic parameters of 20 mg/kg orally administered ceritinib at 3 h and 24 h after administration to male wild-type, *Abcg2*^{-/-}, *Abcb1a/1b*^{-/-} and *Abcb1a/1b;Abcg2*^{-/-} mice.

Parameter	Time (h)	Genotype			
		Wild-type	<i>Abcg2</i> ^{-/-}	<i>Abcb1a/1b</i> ^{-/-}	<i>Abcb1a/1b;Abcg2</i> ^{-/-}
Plasma AUC ₍₀₋₃₎ (μg ml/h)	3	4.4 ± 0.8	3.8 ± 1.1	3.5 ± 0.9	4.0 ± 0.2
Fold change AUC ₍₀₋₃₎		1.0	0.9	0.8	0.9
C _{max} (μg/ml)		2.6 ± 0.7	2.2 ± 0.4	1.9 ± 0.4	2.2 ± 0.5
T _{max} (h)		≥3	≥3	≥3	≥3
C _{brain} (μg/g)		0.06 ± 0.02	0.03 ± 0.02	2.2 ± 0.6 ^{***}	5.2 ± 0.4 ^{**}
Fold change C _{brain}		1.0	0.5	38	90
P _{brain} (10 ⁻³ h ⁻¹)		14 ± 6.2	7.9 ± 5.1	642 ± 114	1303 ± 95 ^{**}
Fold change P _{brain}		1.0	0.6	47	96
Plasma AUC ₍₀₋₂₄₎ (μg ml/h)	24	41 ± 10	38 ± 3.6	39 ± 7.5	37 ± 2.6
Fold change AUC ₍₀₋₂₄₎		1.0	0.9	0.9	0.9
C _{max} (μg/mL)		2.6 ± 0.7	2.1 ± 0.2	2.1 ± 0.5	2.2 ± 0.5
T _{max} (h)		2–8	2–24	2–24	2–24
C _{brain} (μg/g)		0.16 ± 0.01	0.13 ± 0.02 [*]	10 ± 1.6 ^{***}	31 ± 2.1 ^{**}
Fold change C _{brain}		1.0	0.8	62	193
P _{brain} (10 ⁻³ h ⁻¹)		4.1 ± 1.1	3.4 ± 0.5	262 ± 53 ^{***}	845 ± 23 ^{**}
Fold change P _{brain}		1.0	0.8	63	204

AUC—area under the plasma concentration–time curve; C_{max}—maximum drug concentration in plasma; T_{max}—the time (h) after drug administration needed to reach maximum plasma concentration; C_{brain}—brain concentration; P_{brain}—brain accumulation (brain concentration divided by AUC).

*P<0.05; ***P<0.001 compared to WT mice and; #P<0.01; ###P<0.001 for comparison between *Abcb1a/1b*^{-/-} and *Abcb1a/1b;Abcg2*^{-/-} mice. Data are given as mean ± SD (n=4–6).

Fig. 3a). Similar effects were observed when brain-to-plasma ratios or brain accumulation (brain concentration divided by plasma AUC) were plotted, indicating that *Abcg2* had a significant effect on ceritinib brain penetration, but only detectable in the absence of *Abcb1a/1b* (Fig. 3a–c).

We next studied the impact of the transporters on brain accumulation of ceritinib at 3 h after oral administration, corresponding roughly with the end of the absorption phase. Similar plasma concentrations to the previous experiment were reached at 3 h, with again no significant differences between the strains (Fig. 2b, Table 1). Ceritinib concentrations in brains of wild-type, *Abcg2*^{-/-}, *Abcb1a/1b*^{-/-}, and *Abcb1a/1b;Abcg2*^{-/-} mice showed similar profiles compared to the 24 h experiment (Fig. 4a, Table 1). However, the brain concentrations were 3 to 6-fold lower than at 24 h, indicating ongoing ceritinib accumulation in the brain of all mouse strains after 3 h (Fig. 4a, Table 1). This is probably a consequence of the prolonged residence of ceritinib in plasma of these strains, and suggests continued availability of plasma ceritinib for distribution into tissues. This was further supported by comparing the 3 and 24 h brain-to-plasma ratios (Figs. 3 and 4b). Also the 3 h brain-to-plasma ratios and brain accumulation data yielded similar profiles for the four strains as the 24 h experiment (Fig. 4a–c, Table 1). Altogether

this indicates that *Abcb1a/1b* is primarily responsible for the strong restriction in ceritinib brain accumulation, taking over most of the restrictive function of *Abcg2* in the BBB in the single *Abcg2*^{-/-} mice. This means that *Abcg2* in the BBB does transport ceritinib *in vivo*, but that this becomes only apparent when *Abcb1a/1b* is absent.

3.4. Effects of *Abcb1a/1b* and *Abcg2* on liver and kidney distribution of ceritinib

We also analyzed the liver and kidney concentrations of ceritinib at 3 and 24 h after oral ceritinib administration (Supplementary Figs. 2 and 3). In contrast to the brain concentrations, we found no relevant differences in tissue concentrations or accumulation after 3 h, and only a modest shift in liver concentration and accumulation, but not kidney concentration and accumulation, of ceritinib at 24 h in both *Abcb1a/1b*-deficient strains (Supplementary Fig. 3). Considering the likely rapid equilibration between plasma and liver, and the higher plasma concentrations of ceritinib in the *Abcb1a/1b*-deficient strains at 24 h, this may simply reflect the higher plasma concentrations in these strains. This was borne out by the virtually identical liver-to-plasma ratios between the strains (Supplementary Fig. 3c). Still, if there is indeed a delayed elimina-

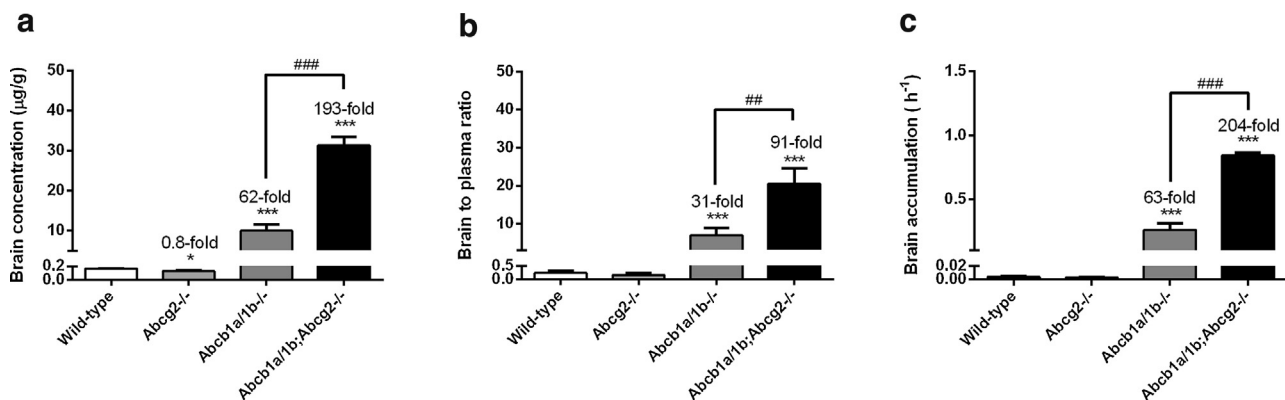


Fig. 3. Brain concentration (a), brain-to-plasma ratio (b) and relative brain accumulation (c) of ceritinib in male wild-type, *Abcg2*^{-/-}, *Abcb1a/1b*^{-/-} and *Abcb1a/1b;Abcg2*^{-/-} mice, 24 h after oral administration of 20 mg/kg ceritinib. *, P<0.05; ***, P<0.001 compared with WT mice and #, P<0.01; ###, P<0.001 for comparison between *Abcb1a/1b*^{-/-} and *Abcb1a/1b;Abcg2*^{-/-} mice. Data are presented as mean ± SD (n=4–5). Where necessary, data were log-transformed to normalize the SDs between study groups for statistical analysis.

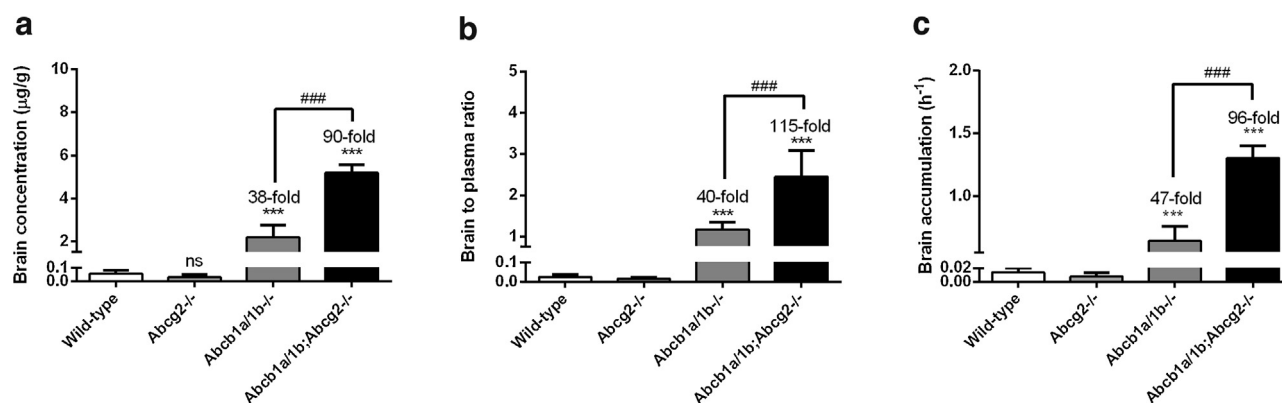


Fig. 4. Brain concentration (a), brain-to-plasma ratio (b) and relative brain accumulation (c) of ceritinib in wild-type, *Abcg2*^{-/-}, *Abcb1a/1b*^{-/-} and *Abcb1a/1b;Abcg2*^{-/-} mice, 3 h after oral administration of 20 mg/kg ceritinib. ***, *P* < 0.001 compared with WT mice and ###, *P* < 0.001 for comparison between *Abcb1a/1b*^{-/-} and *Abcb1a/1b;Abcg2*^{-/-} mice. Data are presented as mean ± SD (*n* = 4–6). Where necessary, data were log-transformed to normalize the SDs between study groups for statistical analysis.

tion of ceritinib in the *Abcb1a/1b*-deficient strains, this would likely involve delayed biliary excretion through the liver because of the absence of bile canalicular *Abcb1a/1b*. The higher liver accumulation of ceritinib in the *Abcb1a/1b*-deficient strains at 24 h would be compatible with this possibility.

4. Discussion

In this study we found that the second generation ALK inhibitor ceritinib is an exceptionally good transport substrate of hABCB1 and a good substrate of hABCG2 and mAbcg2 *in vitro*. Accordingly, upon oral administration of ceritinib to mice, we found very large increases in brain accumulation in *Abcb1a/1b*^{-/-} and *Abcb1a/1b;Abcg2*^{-/-} mice, confirming that these transporter proteins in the BBB actively keep ceritinib out of the brain, with *Abcb1a/1b* playing the dominant role. Additionally, we found that mAbcb1a/1b and mAbcg2 had little or no impact on the oral absorption of ceritinib but the prolonged high plasma concentrations in *Abcb1a/1b*-deficient strains suggest that *Abcb1a/1b* may play a role in the later plasma clearance of the drug. Liver and kidney accumulation of ceritinib were not strongly affected by *Abcb1a/1b* and/or *Abcg2* activity, and mostly in line with the ceritinib plasma concentrations.

Our *in vitro* results show that ceritinib was transported much more efficiently by hABCB1 than by hABCG2, whereas mAbcg2 had an intermediate activity. We note that comparatively low transport by hABCG2 compared to mAbcg2 in our cell lines may have to do with the relative difficulty in obtaining well-growing MDCKII cells with high hABCG2 expression, as discussed previously [28,29]. Moreover, considering that the expression of hABCG2 relative to hABCB1 in the human BBB is 4.3-fold higher than the expression ratio of mAbcg2 and mAbcb1a in the mouse BBB [30], it may well be that ceritinib accumulation in the human brain is in fact more affected by hABCG2 relative to hABCB1 activity than would be suggested by the current mouse brain accumulation data.

Importantly, after oral administration at 20 mg/kg, we obtained ceritinib plasma levels in the same range as the steady state concentrations reported in man [19]. This suggests that the brain and tissue accumulation conditions that applied in the mice in our study were similar to those relevant for human patients. The ceritinib absorption phase in all tested mouse strains was comparable, indicating that the oral availability of ceritinib is not hindered by intestinal efflux by either mAbcb1a/1b or mAbcg2 in mice (Fig. 2a and b). This is consistent with previous reports for many other tyrosine kinase inhibitors that are good *Abcb1a/1b* and/or *Abcg2* substrates such as sorafenib [28], regorafenib [29], dasatinib [31] and CYT387 [29,32]. We cannot exclude the theoretical possibility, though, that the very

high concentration of ceritinib obtained in the intestinal lumen shortly after oral administration may have saturated or inhibited the intestinal ABC transporters. Even though ceritinib was not fully eliminated within 24 h, the decline in ceritinib plasma concentrations in *Abcb1a/1b*-deficient strains seemed slower compared to that in wild-type mice. This would suggest that *Abcb1a/1b* may play a role in the elimination of ceritinib. Absence of this efflux protein might thus result in a prolonged systemic exposure to ceritinib. Even in wild-type mice, elimination of ceritinib from plasma and major organs such as liver and kidney appeared to be very slow (Fig. 2, Supplementary Figs. 2 and 3). This suggests that there are no other efficient ceritinib-clearing mechanisms in mice. Also the main human cytochrome P450 enzymes such as CYP3A4 and CYP2C9 show only modest metabolic conversion of ceritinib *in vitro* [21].

Similar to crizotinib and many other TKI's, ceritinib is a dual *Abcb1a/1b* and *Abcg2* substrate and it is subject to a collaborative action of these proteins at the BBB [33]. This effect has previously been described and explained extensively using theoretical pharmacokinetic models [34,35]. The *in vivo* finding that *Abcg2* has no detectable effect on ceritinib brain penetration in the presence of *Abcb1a/1b* is again consistent with reports for crizotinib and many other tyrosine kinase inhibitors that are shared *Abcb1a* and *Abcg2* substrates. One explanation for this is a relatively more modest amount of *Abcg2* proteins expressed at the mouse BBB in relation to mAbcb1a/1b, next to the fact that we have shown that *in vitro* hABCB1 is a considerably more efficient transporter for ceritinib than hABCG2 and mAbcg2 [30].

Setting aside the active transport of ceritinib by *Abcb1a/1b* and to a lesser extent mAbcg2, we found that ceritinib on itself is still capable of penetrating the wild-type BBB, albeit at low concentrations (brain-to-plasma ratio is well below 0.3, Figs. 3 and 4). It could be that an as yet unidentified uptake transporter at the BBB helps to transport ceritinib into the brain, or perhaps that the lipophilicity of ceritinib allows the molecule to diffuse through the BBB at a significant rate. Nonetheless, considering the strong impact of *Abcb1a/1b* and *Abcg2* on brain accumulation of ceritinib, we think our results might provide a basis for cotreatment of ceritinib with single or dual ABCB1 and ABCG2 inhibitors to improve the treatment of brain (micro) metastases positioned in part or in whole behind a functionally intact BBB, or possibly of tumors overexpressing ABCB1 and/or ABCG2.

5. Conclusion

We have shown that the second generation ALK inhibitor ceritinib is transported very efficiently by hABCB1 and efficiently by

mAbcg2 and hABCG2 *in vitro*. This is supported by our *in vivo* data displaying an impressive increase in brain penetration in Abcb1a/1b and combined Abcb1a/1b and Abcg2 knockout mice. Our data suggest that coadministration of ceritinib with a dual ABCB1 and ABCG2 inhibitor may improve treatment of tumors resistant to ceritinib due to ABCB1 or ABCG2 overexpression, as well as brain (micro) metastases positioned behind a functionally intact blood-brain barrier.

Conflict of interest

The research group of A.H. Schinkel receives revenue from commercial distribution of some of the mouse strains used in this study. The other authors declare no conflict of interest.

Acknowledgements

We thank Stéphanie van Hoppe for assistance with *in vivo* work and for critical reading of the manuscript. This work was supported by internal funds within The Netherlands Cancer Institute.

Appendix A. Supplementary data

Supplementary data associated with this article can be found, in the online version, at <http://dx.doi.org/10.1016/j.phrs.2015.09.003>.

References

- [1] R.L. Siegel, K.D. Miller, A. Jemal, Cancer statistics, 2015, *CA Cancer J. Clin.* 65 (2015) 5–29, <http://dx.doi.org/10.3322/caac.21254>.
- [2] J.D. Johnson, B. Young, Demographics of brain metastasis, *Neurosurg. Clin. N. Am.* 7 (1996) 337–344.
- [3] A. Bollmann, T. Blankenburg, J. Haerting, O. Kuss, W. Schutte, J. Dunst, et al., Survival of patients in clinical stages I–IIIb of non-small-cell lung cancer treated with radiation therapy alone. Results of a population-based study in Southern Saxony-Anhalt, *Strahlenther. Onkol.* 180 (2004) 488–496, <http://dx.doi.org/10.1007/s00066-004-1184-7>.
- [4] A. Fabi, A. Felici, G. Metro, A. Mirri, E. Bria, S. Telera, et al., Brain metastases from solid tumors: disease outcome according to type of treatment and therapeutic resources of the treating center, *J. Exp. Clin. Cancer Res.* 30 (2011) 10, <http://dx.doi.org/10.1186/1756-9966-30-10>.
- [5] T.J. Lynch, D.W. Bell, R. Sordella, S. Gurubhagavatula, R.A. Okimoto, B.W. Brannigan, et al., Activating mutations in the epidermal growth factor receptor underlying responsiveness of non-small-cell lung cancer to gefitinib, *N. Engl. J. Med.* 350 (2004) 2129–2139, <http://dx.doi.org/10.1056/NEJMoa040938>.
- [6] J.G. Paez, P.A. Janne, J.C. Lee, S. Tracy, H. Greulich, S. Gabriel, et al., EGFR mutations in lung cancer: correlation with clinical response to gefitinib therapy, *Science* 304 (2004) 1497–1500, <http://dx.doi.org/10.1126/science.1099314>.
- [7] M. Soda, Y.L. Choi, M. Enomoto, S. Takada, Y. Yamashita, S. Ishikawa, et al., Identification of the transforming EML4-ALK fusion gene in non-small-cell lung cancer, *Nature* 448 (2007) 561–566, <http://dx.doi.org/10.1038/nature05945>.
- [8] M. Soda, S. Takada, K. Takeuchi, Y.L. Choi, M. Enomoto, T. Ueno, et al., A mouse model for EML4-ALK-positive lung cancer, *Proc. Natl. Acad. Sci. U. S. A.* 105 (2008) 19893–19897, <http://dx.doi.org/10.1073/pnas.0805381105>.
- [9] X. Zhang, S. Zhang, X. Yang, J. Yang, Q. Zhou, L. Yin, et al., Fusion of EML4 and ALK is associated with development of lung adenocarcinomas lacking EGFR and KRAS mutations and is correlated with ALK expression, *Mol. Cancer* 9 (2010) 188, <http://dx.doi.org/10.1186/1476-4598-9-188>.
- [10] D.R. Camidge, Y.J. Bang, E.L. Kwak, A.J. Iafrate, M. Varella-Garcia, S.B. Fox, et al., Activity and safety of crizotinib in patients with ALK-positive non-small-cell lung cancer: updated results from a phase 1 study, *Lancet Oncol.* 13 (2012) 1011–1019, [http://dx.doi.org/10.1016/S1470-2045\(12\)70344-3](http://dx.doi.org/10.1016/S1470-2045(12)70344-3).
- [11] H. Kaneda, I. Okamoto, K. Nakagawa, Rapid response of brain metastasis to crizotinib in a patient with ALK rearrangement-positive non-small-cell lung cancer, *J. Thorac. Oncol.* 8 (2013) e32–e33, <http://dx.doi.org/10.1097/JTO.0b013e3182843771>.
- [12] Y. Kinoshita, Y. Koga, A. Sakamoto, K. Hidaka, Long-lasting response to crizotinib in brain metastases due to EML4-ALK-rearranged non-small-cell lung cancer, *BMJ Case Rep.* (2013) 2013, <http://dx.doi.org/10.1136/bcr-2013-200867>.
- [13] D. Maillet, I. Martel-Lafay, D. Arpin, M. Perol, Ineffectiveness of crizotinib on brain metastases in two cases of lung adenocarcinoma with EML4-ALK rearrangement, *J. Thorac. Oncol.* 8 (2013) e30–e31, <http://dx.doi.org/10.1097/JTO.0b013e318288dc2d>.
- [14] D.B. Costa, A.T. Shaw, S.H. Ou, B.J. Solomon, G.J. Riely, M.J. Ahn, et al., Clinical experience with crizotinib in patients with advanced ALK-rearranged non-small-cell lung cancer and brain metastases, *J. Clin. Oncol.* (2015), <http://dx.doi.org/10.1200/JCO.2014.59.0539>.
- [15] M.M. Awad, R. Katayama, M. McTigue, W. Liu, Y.L. Deng, A. Brooun, et al., Acquired resistance to crizotinib from a mutation in CD74-ROS1, *N. Engl. J. Med.* 368 (2013) 2395–2401, <http://dx.doi.org/10.1056/NEJMoa1215530>.
- [16] C.A. Perez, M. Velez, L.E. Raez, E.S. Santos, Overcoming the resistance to crizotinib in patients with non-small cell lung cancer harboring EML4/ALK translocation, *Lung Cancer* 84 (2014) 110–115, <http://dx.doi.org/10.1016/j.lungcan.2014.02.001>.
- [17] L. Friboulet, N. Li, R. Katayama, C.C. Lee, J.F. Gainor, A.S. Crystal, et al., The ALK inhibitor ceritinib overcomes crizotinib resistance in non-small cell lung cancer, *Cancer Discov.* 4 (2014) 662–673, <http://dx.doi.org/10.1158/2159-8290.CD-13-0846>.
- [18] T.H. Marsilje, W. Pei, B. Chen, W. Lu, T. Uno, Y. Jin, et al., Synthesis, structure–activity relationships, and *in vivo* efficacy of the novel potent and selective anaplastic lymphoma kinase (ALK) inhibitor 5-chloro-N2-(2-isopropoxy-5-methyl-4-(piperidin-4-yl)phenyl)-N4-(2-(isopropylsulfonyl)phenyl)pyrimidine-2,4-diamine (LDK378) currently in phase 1 and phase 2 clinical trials, *J. Med. Chem.* 56 (2013) 5675–5690, <http://dx.doi.org/10.1021/jm400402q>.
- [19] A.T. Shaw, D.W. Kim, R. Mehra, D.S. Tan, E. Felip, L.Q. Chow, et al., Ceritinib in ALK-rearranged non-small-cell lung cancer, *N. Engl. J. Med.* 370 (2014) 1189–1197, <http://dx.doi.org/10.1056/NEJMoa1311107>.
- [20] S.C. Tang, L.N. Nguyen, R.W. Sparidans, E. Wagenaar, J.H. Beijnen, A.H. Schinkel, Increased oral availability and brain accumulation of the ALK inhibitor crizotinib by coadministration of the P-glycoprotein (ABCB1) and breast cancer resistance protein (ABCG2) inhibitor elacridar, *Int. J. Cancer* 134 (2014) 1484–1494, <http://dx.doi.org/10.1002/ijc.28475>.
- [21] Center for Drug Evaluation and Research of the US Department of Health and Human Services, Food and Drug Administration, Clinical Pharmacology and Biopharmaceutics Review(s). 2014 [cited 2015 May 8]; Available from: http://www.accessdata.fda.gov/drugsatfda_docs/nda/2014/205755Orig1s000ClinPharmR.pdf.
- [22] R. Evers, M. Kool, L. van Deemter, H. Janssen, J. Calafat, L.C. Oomen, et al., Drug export activity of the human canalicular multispecific organic anion transporter in polarized kidney MDCK cells expressing cMOAT (MRP2) cDNA, *J. Clin. Invest.* 101 (1998) 1310–1319, <http://dx.doi.org/10.1172/jci119886>.
- [23] S. Durmus, R.W. Sparidans, E. Wagenaar, J.H. Beijnen, A.H. Schinkel, Oral availability and brain penetration of the B-RAFV600E inhibitor vemurafenib can be enhanced by the P-GLYCOPROTEIN (ABCB1) and breast cancer resistance protein (ABCG2) inhibitor elacridar, *Mol. Pharm.* 9 (2012) 3236–3245, <http://dx.doi.org/10.1021/mp3003144>.
- [24] A.H. Schinkel, E. Wagenaar, C.A. Mol, L. van Deemter, P-glycoprotein in the blood–brain barrier of mice influences the brain penetration and pharmacological activity of many drugs, *J. Clin. Invest.* 97 (1996) 2517–2524, <http://dx.doi.org/10.1172/jci118699>.
- [25] J.W. Jonker, M. Buitelaar, E. Wagenaar, M.A. Van Der Valk, G.L. Scheffer, R.J. Scheper, et al., The breast cancer resistance protein protects against a major chlorophyll-derived dietary phototoxin and protoporphyria, *Proc. Natl. Acad. Sci. U. S. A.* 99 (2002) 15649–15654, <http://dx.doi.org/10.1073/pnas.202607599>.
- [26] J.W. Jonker, J. Freeman, E. Bolscher, S. Musters, A.J. Alvi, I. Titley, et al., Contribution of the ABC transporters Bcrp1 and Mdr1a/1b to the side population phenotype in mammary gland and bone marrow of mice, *Stem Cells* 23 (2005) 1059–1065, <http://dx.doi.org/10.1634/stemcells.2005-0150>.
- [27] H. Dai, P. Marbach, M. Lemaire, M. Hayes, W.F. Elmquist, Distribution of STI-571 to the brain is limited by P-glycoprotein-mediated efflux, *J. Pharmacol. Exp. Ther.* 304 (2003) 1085–1092, <http://dx.doi.org/10.1124/jpet.102.045260>.
- [28] J.S. Lagas, R.A. van Waterschoot, R.W. Sparidans, E. Wagenaar, J.H. Beijnen, A.H. Schinkel, Breast cancer resistance protein and P-glycoprotein limit sorafenib brain accumulation, *Mol. Cancer Ther.* 9 (2010) 319–326, <http://dx.doi.org/10.1158/1535-7163.MCT-09-0663>.
- [29] A. Kort, S. Durmus, R.W. Sparidans, E. Wagenaar, J.H. Beijnen, A.H. Schinkel, Brain and testis accumulation of regorafenib is restricted by breast cancer resistance protein (BCRP/ABCG2) and P-glycoprotein (P-GP/ABCB1), *Pharm. Res.* (2015), <http://dx.doi.org/10.1007/s11095-014-1609-7>.
- [30] Y. Uchida, S. Ohtsuki, Y. Katsukura, C. Ikeda, T. Suzuki, J. Kamiie, et al., Quantitative targeted absolute proteomics of human blood–brain barrier transporters and receptors, *J. Neurochem.* 117 (2011) 333–345, <http://dx.doi.org/10.1111/j.1471-4159.2011.07208.x>.
- [31] J.S. Lagas, R.A. van Waterschoot, V.A. van Tilburg, M.J. Hillebrand, N. Lankheet, H. Rosing, et al., Brain accumulation of dasatinib is restricted by P-glycoprotein (ABCB1) and breast cancer resistance protein (ABCG2) and can be enhanced by elacridar treatment, *Clin. Cancer Res.* 15 (2009) 2344–2351, <http://dx.doi.org/10.1158/1078-0432.CCR-08-2253>.
- [32] S. Durmus, N. Xu, R.W. Sparidans, E. Wagenaar, J.H. Beijnen, A.H. Schinkel, P-glycoprotein (MDR1/ABCB1) and breast cancer resistance protein (BCRP/ABCG2) restrict brain accumulation of the JAK1/2 inhibitor, CYT387, *Pharmacol. Res.* 76 (2013) 9–16, <http://dx.doi.org/10.1016/j.phrs.2013.06.009>.

- [33] S. Agarwal, A.M. Hartz, W.F. Elmquist, B. Bauer, Breast resistance protein and P-glycoprotein in brain cancer: two gatekeepers team up, *Curr. Pharm. Des.* 17 (2011) 2793–2802, <http://dx.doi.org/10.2174/138161211797440186>.
- [34] J.C. Kalvass, G.M. Pollack, Kinetic considerations for the quantitative assessment of efflux activity and inhibition: implications for understanding and predicting the effects of efflux inhibition, *Pharm. Res.* 24 (2007) 265–276, <http://dx.doi.org/10.1007/s11095-006-9135-x>.
- [35] H. Kodaira, H. Kusuhara, J. Ushiki, E. Fuse, Y. Sugiyama, Kinetic analysis of the cooperation of P-glycoprotein (P-gp/Abcb1) and breast cancer resistance protein (Bcrp/Abcg2) in limiting the brain and testis penetration of erlotinib, flavopiridol, and mitoxantrone, *J. Pharmacol. Exp. Ther.* 333 (2010) 788–796, <http://dx.doi.org/10.1124/jpet.109.162321>.